LITERATURE CITED

1. G. M. Lyakhov, "Shock waves in multicomponent media," Izv. Akad. Nauk SSSR, Mekh. Mashinostr., No. 1 (1959).
2. G. M. Lyakhov, Waves in Soils and Porous Multicomponent Media [in Russian], Nauka, Moscow (1982).
3. G. M. Lyakhov and G. B. Frash, "Blast waves in frozen soils," Zh. Prikl. Mekh. Tekh. Fiz., No. 6 (1983).
4. V. A. Fomin, A Study of Ice Fracture under High Deformation Rates [in Russian], Aerodynamic and Geocosmic Studies, MFTI, Moscow (1984).
5. V. A. Fomin and V. N. Rodionov, "On the dissipation of mechanical energy on ice," Dokl. Akad. Nauk SSSR, 285, No. 6 (1985).
6. L. Hald and N. Sinha, "Rheological behavior of ice under small deformations," in: Physics and Mechanics of Ice [Russian translation], Mir, Moscow (1983).
7. N. K. Sinha, "Rheology of columnar-grained ice," Exp. Mech., 18, No. 12 (1978).
8. N. E. Haskin, "Method of characteristics for the solution of equations of one-dimensional unsteady flow," in: Computational Methods in Hydrodynamics [Russian translation], Mir, Moscow (1971).

STRAIN-HARDENING OF STEEL BY DYNAMIC UNIAXIAL TENSION

A. G. Ivanov, A. I. Korshunov,
A. M. Podurets, V. A. Ryzhanskii,
and N. A. Yukina

UDC 539.375.5

As is well known, many structural materials are sensitive to loading history to some extent. One manifestation of such sensitivity is the strain-hardening of steel as a result of plastic deformation – so-called work-hardening. It was shown in [1] that work-hardening increases with an increase in strain rate. It was established in [2] that in the uniaxial tension of austenitic steel 12Kh18N10T in different rate regimes, the mechanical properties of the steel are significantly affected by factors related to its loading history (particularly relaxation processes and dynamic work-hardening).

The present study (a continuation of [2]) is devoted to examination of the changes in the physicomechanical properties of steel 12Kh18N10T as a result of its dynamic tension.

The material for our study was taken from a cylindrical shell (outside radius R_0, thickness $0.0246R_0$, length $4R_0$) welded from steel plates which were quenched and cooled in air. The shell was filled with water and was twice loaded by a spherical charge of high explosive (HE) detonated at the center. In each explosion, the charge itself was placed at the geometric center of the shell. The tests were conducted in open air. The temperature of the water-filled shell in the tests was (293 ± 5) K. The shell was deformed into a box shape as a result of the explosions. Measurement showed that the strains of the shell were close to uniaxial: with radial expansion, its considerable circumferential tension (about 40% in the central cross section) was accompanied by thinning and slight (maximum of about 3% in the same section) contraction along the generatrix. The results of high-speed photographs taken in the tests by the shadow method [3] showed that the shell pulsated slightly as it expanded (due to the action of compression waves circulated in the water, which is typical of underwater explosions [4]).

The test specimens were cut in three shell regions located at different sites and, thus, characterized by different loading histories: in the region of the central cross section A, closest to the center of the explosion (where the strain rate was therefore the highest), the circumferential plastic strain ε_0 was about 37%; in region B, located between region A and the edge of the shell, $\varepsilon_0 \approx 17\%$; in region C at the edge of the shell, where the strain rate was lowest, $\varepsilon_0 \approx 2\%$. The machining performed during cutting of the semifinished products and preparation of the specimens was done in regimes which kept it from affecting the properties of the material.

Moscow. Translated from Zhurnal Prikladnoi Mekhaniki i Tekhnicheskoi Fiziki, No. 6, pp. 133-140, November-December, 1987. Original article submitted June 4, 1986.

0021-8944/87/2806-0923$12.50

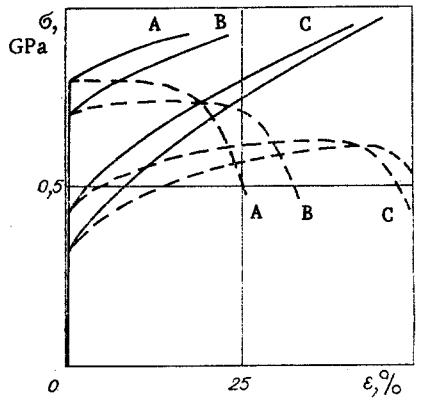

Fig. 1

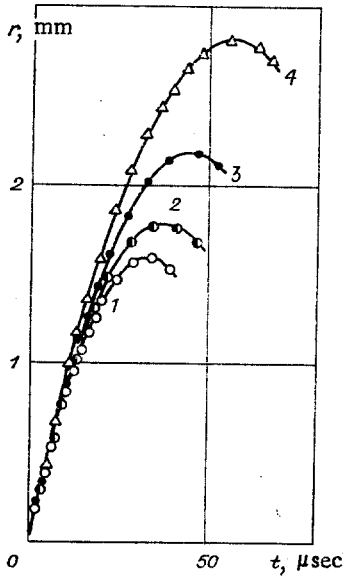

Fig. 2

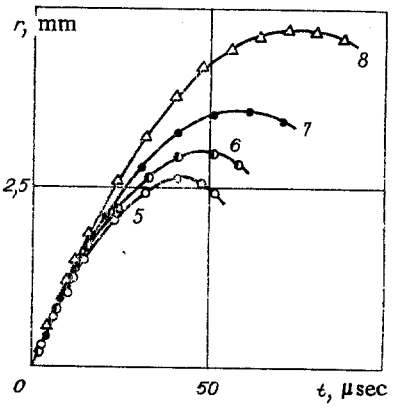

Fig. 3

TABLE 1

Region	ε_0, %	$\sigma_{0,2}$, GPa	σ_u, GPa	δ, %
A	37	0,797	0,808	24
B	17	0,701	0,749	32
C	2	0,424	0,632	51
Initial state	0	0,341	0,582	52

The specimens were tested at a temperature of (288 ± 5) K. We determined the mechanical properties of the steel both in the above-mentioned regions of the shell and in the initial, undeformed shell. We also studied the microstructure of the steel.

Static tests were conducted on cylindrical specimens prepared in accordance with GOST 1497-73 (type IV, No. 6), so that the axes of the specimens were oriented about the circumference of the shell. The plastic strain rate was about 10^{-3} sec^{-1}. After mathematical analysis of machine-generated stress-strain curves of the specimens in tension by the method in [5], we obtained nominal static stress-strain curves for each shell region. These curves are shown by the dashed lines in Fig. 1, where the regions have been indicated as well. The curves without indices are for the material in the initial state. The solid lines show the relations $\sigma(\varepsilon)$, which are similarly indexed (σ is the true stress and ε is the true strain). The solid curves were obtained by recalculating the nominal stress-strain curves with the assumption that the volume undergoing deformation was constant [6] and with allowance for the correction recommended in [7] for the section of the curve located after the formation of the neck on the specimen. The standard mechanical characteristics of the steel are shown in Table 1. The relative errors of the stress and strain determinations were no greater than 1.5 and 3%.

The dynamic tests were conducted in the regime of variable (decreasing from a maximum to zero) strain rate* by the method of impulsive expansion of ring specimens (R_0 = 50 mm, thickness 1 mm, height 3 mm), as in [2]. An initial velocity v_0 was imparted to the ring from inside by a short (0.2 μsec) shock delivered by means of an explosive device [8]. The ring subsequently expanded symmetrically due to inertia, with the expansion slowing as a result of the hoop stress

$$\sigma = -\rho R dv/dt. \qquad (1)$$

Here, ρ is the density of the material; R and v = dR/dt are the running values of the outside radius and the radial velocity of the expanding ring; t is the time of expansion. In the test, we recorded the relations $r(t) = R(t) - R_0$. These results are shown by the points in Figs. 2 and 3. The numbers of the curves correspond to the numbers of the tests in Table 2,

*This regime is close to the regime of deformation of the shell when it is loaded by internal explosion.

TABLE 2

Test series	Region	No. of test	v_0, m/sec	$\dot{\varepsilon}_0$, sec^{-1}	ε_1, %	t_1, μsec	σ, GPa
I	A	1	98,1	1962	3,2	33,0	1,184
	B	2	98,0	1960	3,5	37,0	1,057
	C	3	98,2	1964	4,3	45,2	0,872
	Initial state	4	97,4	1948	5,5	59,0	0,668
II	A	5	128,8	2576	5,4	43,4	1,199
	B	6	128,4	2568	6,0	48,4	1,077
	C	7	129,6	2592	7,2	58,5	0,907
	Initial state	8	130,0	2600	9,0	74,0	0,728

where $\dot{\varepsilon}_0 = v_0/R_0$ is the initial rate of circumferential deformation of the ring and ε_1 and t_1 are the maximum circumferential strain and the time required to attain it. The relative errors of v_0, ε_1, and t_1 are no greater than 7, 5, and 2%, respectively.

The stress state of the ring was analyzed by the method in [2]. In accordance with this method, at $0 \le t \le t_1$,* with the assumption

$$\sigma(\varepsilon) = \sigma = \text{const} \tag{2}$$

we write the integrals of Eq. (1) as follows

$$\dot{\varepsilon}(\varepsilon) = \dot{\varepsilon}_0 \sqrt{1 - \varepsilon/\varepsilon_1}\exp(-\varepsilon); \tag{3}$$

$$E(\varepsilon) = CT(t); \tag{4}$$

$$\varepsilon = \ln(1 + r/R_0), \quad \varepsilon_1 = \rho v_0^2/2\sigma; \tag{5}$$

$$E(\varepsilon) = \sum_{n=1}^{\infty}(-1)^{n-1} a_n (1 - \varepsilon/\varepsilon_1)^{(2n-1)/2}; \tag{6}$$

$$T(t) = 1 - t/t_1; \tag{7}$$

$$C = \dot{\varepsilon}_0 t_1/2\varepsilon_1. \tag{8}$$

Equation (4) was found by replacing the exponent in (3) by a Taylor series. At n = 4 (relative error no less than 0.01%), the coefficients in (6) have the form

$$a_1 = 1 + \varepsilon_1 + \varepsilon_1^2/2 + \varepsilon_1^3/6, \quad a_2 = (1 + \varepsilon_1 + \varepsilon_1^2/2)\varepsilon_1, \tag{9}$$
$$a_3 = (1 + \varepsilon_1)\varepsilon_1^2/2, \quad a_4 = \varepsilon_1^3/6.$$

Thus, a linear relationship between the functionals (6) and (7) is the criterion of the validity of assumption (2). Within the framework of the well-known model of a rigid-viscoplastic body

$$\sigma = \sigma_0 + k\varepsilon + \eta\dot{\varepsilon} \tag{10}$$

(σ_0 is the static yield point, k is the strain-hardening coefficient, η is the absolute viscosity), this statement means physically that the strain-hardening occurring in the ring as it expands under the influence of inertial forces, with an increase in ε, is offset by softening which occurs as $\dot{\varepsilon}$ decreases due to deceleration of the ring's expansion.

Equation (4), obtained from the experimental points of r(t), is very close to linear. This has made it possible to conclude that in tests with $0 \le t \le t_1$ (within the limits of the empirical error), a stress state of type (2) was realized in the rings. Furthermore, in accordance with (5),

$$\sigma = \rho v_0^2/2\varepsilon_1. \tag{11}$$

The lines in Figs. 2 and 3 show calculated relations r(t) found from formulas which follow from (4)-(9). The calculated results agree quite satisfactorily with the experimental results. The relations $\dot{\varepsilon}(\varepsilon)$ and $\sigma(\varepsilon)$ found from Eqs. (3) and (11) are shown in Fig. 4 with numbers corresponding to the numbers of the tests in Table 2. This table also gives values of σ (error no greater than 10%).

*The interval $0 \le t \le t_1$ is of the greatest interest, since the maximum drop in strain rate occurs within it.

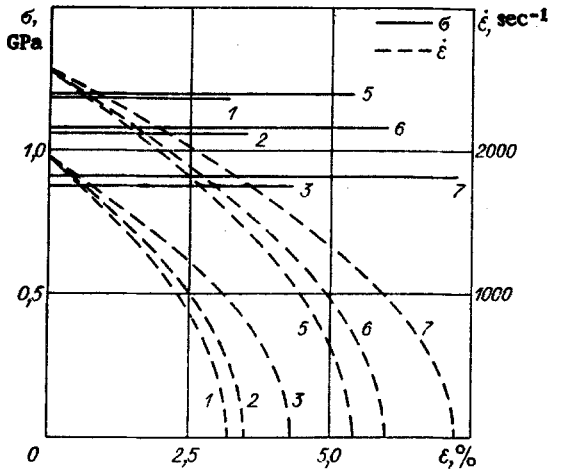

Fig. 4

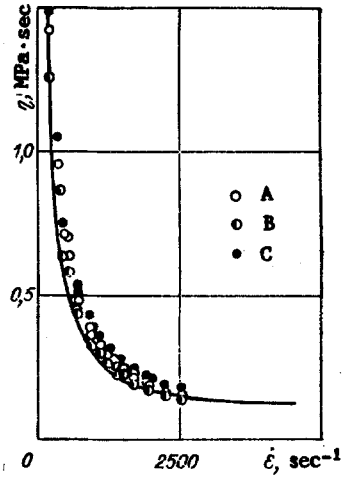

Fig. 5

TABLE 3

Region	k, GPa			
	Statics	Dynamics		
		$\dot{\varepsilon}$		
	$\dot{\varepsilon} \approx 10^{-3}$ sec^{-1}	$2 \cdot 10^3$ sec^{-1}	10^3 sec^{-1}	0
A	0,70	0,73	0,64	0,69
B	0,87	0,86	0,83	0,82
C	1,16	1,25	1,21	1,20
Initial state	1,38	1,40	1,40	1,40

By using Fig. 4 as a nomogram, we can change over from $\sigma(\varepsilon)$ with variable $\dot{\varepsilon}$ to $\sigma(\varepsilon)$ with $\dot{\varepsilon}$ = const.* As in [2], their graphs are straight lines with the slopes k. Values of these slopes, evaluated for several values of $\dot{\varepsilon}$, are shown in Table 3. Also shown for comparison are values of k evaluated from the static relations $\sigma(\varepsilon)$ in Fig. 1.

It follows from the results obtained that, other conditions being equal, the dynamically deformed steel specimens exhibit clear changes in mechanical properties from the initial state. For example, in static tension, there is an increase in strengths $\sigma_{0.2}$ and σ_u and a reduction in ductility δ (see Table 1 and Fig. 1). In dynamic tension, there is a reduction in compliance which is manifest in a decrease in the amplitude of the strain of the ring ε_1 and an increase in the dynamic stresses (see Table 2 and Figs. 2-4). This is evidence of work-hardening in the steel of the shell.

It was shown in [2] that the degree of strain-hardening of steel depends not only on the level of dynamic strain, but also on the rate regime of the deformation. Our results are consistent with this conclusion. In fact, the greatest work-hardening is seen in the region A, closest to the center of the explosion. Deformation in this region took place with the greatest rate gradient. Thus, the yield strength of the steel in this part of the specimen increased by a factor of about 2.3 compared to the initial state. The pulsating character of the shell expansion evidently facilitated its strain-hardening. With increasing distance from region A toward the edge of the shell, the strain rates decreased, with a corresponding reduction in work-hardening. Thus, in region B, the yield strength increased by a factor of about two, i.e., less than in region A, while in region C – where the strain and strain rate were minimal – work-hardening was negligible. The yield strength in region C increased by a total of only 30%. The above-noted reduction in δ with an increase in the plastic strain of the shell is a manifestation of a natural reduction in the ductility reserves of the steel as a result of its tension and, as the mechanical factors, serves to characterize the degree of work-hardening.

*In Fig. 4, it is necessary to draw a horizontal line through the prescribed value of $\dot{\varepsilon}$ = const and to project the points of its intersection with the curves $\dot{\varepsilon}(\varepsilon)$ for each test on the corresponding relations $\sigma(\varepsilon)$ and the axis ε. These projections are the coordinates (σ, ε) of the points of the sought relation.

TABLE 4

Region	α-phase, %: inside surface	inside layer	middle layer	outside layer	Outside surface
A	55	25	15	15	40
B	40	20	20	10	30
C	40	20	20	10	25

TABLE 5

Region	$HV_{0,05}$, GPa: min	max	mean	B, T
A	2,92	4,20	3,45	76
B	2,76	3,87	3,29	51
C	2,10	2,96	2,43	44
Initial state	1,83	2,04	1,92	25

It should be noted that (see Table 3) the strain-hardening coefficient k of the steel is nearly insensitive to strain rate (in the investigated range of strain rate) but does depend on the work-hardening: with a decrease in ε_0, i.e., as work-hardening decreases, k increases significantly and approaches its values for the steel in the initial state. To evaluate the possible character of $k(\varepsilon_0)$, we will examine a rheological equation more general than Eq. (10). The new equation was derived [9] on the basis of the dislocational model of plastic flow:

$$\sigma = \sigma_0 + \int\limits_{(\varepsilon)} [M(\varepsilon, \dot{\varepsilon}) - N(\varepsilon, \dot{\varepsilon})/\dot{\varepsilon}]\, d\varepsilon + \int\limits_{(\dot{\varepsilon})} \mu(\varepsilon, \dot{\varepsilon})\, d\dot{\varepsilon}, \tag{12}$$

where M and N are the strain-hardening and softening moduli; μ is the viscosity of the material. The second term in (12) is obvious an analog of the second term in (10). By definition, $k = \partial\sigma/\partial\varepsilon$. Thus

$$k = M(\varepsilon, \dot{\varepsilon}) - N(\varepsilon, \dot{\varepsilon})/\dot{\varepsilon}. \tag{13}$$

Having compared the dimensions of M and N in (13), as a first approximation we take $N \sim \dot{\varepsilon}$. Considering the closeness of the rate regimes in the expansion of the ring and shell, we assume – despite the pulsation of the shell's expansion – that for the shell too the relation $\dot{\varepsilon}(\varepsilon)$ is on the average exponential in character and is of the type (3). Thus, $N \sim \exp \times (-\varepsilon)$, and the relation $k(\varepsilon_0)$ may also be exponential. Having followed this approach and analyzed the data in Table 3 by the least squares method, we obtain $k(\varepsilon_0) = 1.4 \exp(-1.2\sqrt{\varepsilon_0})$, GPa.

By using values of k from Table 3 averaged for the different regions and taking the relations $\sigma(\varepsilon)$ and $\dot{\varepsilon}(\varepsilon)$ from Fig. 4, we can evaluate the absolute viscosity of the steel in each region by a formula which follows from (10): $\eta(\dot{\varepsilon}) = (\sigma - \sigma_0 - k\varepsilon)/\dot{\varepsilon}$. The resulting values of $\eta(\dot{\varepsilon})$ at $\sigma_0 = \sigma_{0.2}$, $\dot{\varepsilon} \lesssim 2600$ sec^{-1} and ε = 1-9% are shown by the points in Fig. 5 and are obviously close to the relation $\eta(\dot{\varepsilon})$ found in [2] for this steel in the initial state (line). This means that the absolute viscosity of the steel is nearly independent of the degree of work-hardening.

The microstructure of the steel was studied by the methods of x-ray diffraction and metallographic analysis. The magnetic properties were also checked.

The x-ray diffraction study was performed on a URS-50IM unit in radiation from a molybdenum anode. The x-ray tube was operated in the regime U = 30 kV, I = 7 mA. Diffraction patterns were obtained for the inside and outside surfaces of the shell and three layers of equal thickness through the shell wall. The results of analysis of the diffraction patterns are shown in Table 4 in the form of estimates of the relative volumetric content of the α-phase of the Fe–Ni system in the initial γ-phase in specimens from different shell regions. The estimates were obtained from the ratios of the integral intensities of the diffraction peaks of the (110)α- and (111)γ-phases on the diffraction patterns (relative error no greater than 10%).

The metallographic analysis was performed on microsections of the cross section of the shell. The relief of the structure of the shell was revealed by the electrolytic method in concentrated nitric acid. The same microsections were used to measure the hardness of the steel $HV_{0.05}$ with a PMT-3 hardness tester under GOST 9450–76. The specimen was loaded by an indenter weighing 50 g. Measurements were made through the thickness of the shell at different distances from its inside surface. Since the α-phase (in contrast to nonmagnetic γ-phase) imparts ferromagnetic properties to chromium–nickel steel, we used the induction-pulse method on a BU-3 unit, with a magnetic field of about 1990 A/m, to measure magnetic induction B in specially made annular specimens (R_0 = 14 mm, thickness 3 mm, height 5 mm) which

served as the cores of toroidal coils. The measurement results are shown in Table 5 and indicate that there is an appreciable increase in the hardness and permeability of the steel from region C to region A, i.e., as work-hardening increases.

In analyzing the results of study of the steels' microstructure, we should note (see Tables 4 and 5) that some of the α-phase of the Fe–Ni system changed into γ-phase. Here, the content of the α-phase correlates with the degree of work-hardening, since there is a marked tendency for the content of the α-phase to decrease going from the central region of the shell toward the edge. A similar tendency is seen in moving across the shell from the middle to the exterior (excluding the outside surface, where the concentration of the α-phase was higher for some unknown reason). The results of the metallographic analysis also provide evidence of a γ–α-phase transformation: the structure of the steel in the initial state is typical austenite, with its characteristic smooth, light-colored grains and infrequent traces of plastic deformation (evidently from rolling of the sheet). In the shell, the metal is strongly textured and the grains are nonuniform and are speckled with black traces of plastic strain in the form of distinct slip bands. Meanwhile, the relief of the intragranular structure is characteristic of martensite. The presence of martensite can also be detected from the increase in the hardness and permeability of the steel.

As is known, martensitic transformations occur most completely at low temperatures and lead to a significant increase in strength and hardness and a reduction in the ductility of steels [10]. For the phase transition to occur at normal and elevated temperatures, an excess of externally supplied strain energy is needed to overcome potential barriers during the transition [11]. This condition is met either in shock-wave loadings [12, 13] or in the combined loading of an object by a shock wave and high-rate tension [14], as in the present study.

Summaring the results, we can state the following: 1) the dynamic uniaxial tension of steel 12Kh18N10T in a pulsating rate regime results in its work-hardening as a result of deformation and phase transformation, and the degree of work-hardening is directly dependent on the intensity of the shock-wave loading and the dynamism and magnitude of the plastic strain; 2) other conditions being equal, work-hardening significantly increases the strength properties of the steel and lowers its ductility properties compared to the initial state; 3) the strain-hardening coefficient is nearly independent of the strain rate, as reported in [2], but decreases significantly as work-hardening proceeds (this relationship is close to exponential); 4) the absolute viscosity of the steel is nearly independent of the degree of work-hardening, and its dependence on strain rate is close to the analogous dependence for the steel in the initial state.

LITERATURE CITED

1. P. O. Pashkov, "Experimental method in the shaping of metals by shock waves," in: High-Rate Deformation [in Russian], Nauka, Moscow (1971).
2. A. G. Ivanov, Yu. G. Kashaev, et al., "Effect of loading history on the mechanical properties of steel in uniaxial tension," Zh. Prikl. Mekh. Tekh. Fiz., No. 6 (1982).
3. A. S. Dubovik, Photographic Recording of High-Speed Processes [in Russian], Nauka, Moscow (1975).
4. K. P. Stanyukovich (ed.), Physics of Explosion [in Russian], Nauka, Moscow (1975).
5. A. I. Korshunov, T. N. Kravchenko, and O. M. Savel'eva, "Construction of stress–strain curves by recalculation of a machine-generated curve," Probl. Prochn., No. 9 (1982).
6. N. N. Malinin, Applied Theory of Plasticity and Creep [in Russian], Mashinostroenie, Moscow (1975).
7. N. N. Davidenkov and N. I. Spiridonova, "Analysis of the stress state in the neck of a specimen in tension," Zavod. Lab., 11, No. 6 (1945).
8. A. G. Ivanov and V. I. Tsypkin, "Device for studying the dynamic strength properties of materials," Inventor's Certificate, No. 855430 USSR, Otkrytiya. Izobreteniya, No. 21 (1981).
9. G. V. Stepanov, Elastoplastic Deformation of Materials under Shock Loads [in Russian], Naukova Dumka, Kiev (1979).
10. T. N. Shinkarenko, V. G. Khoroshailov, and I. S. Dimchuk, "Dependence of the mechanical properties of austenitic steels 1Kh18N10T and 4Kh12N8G8MFB on low-temperature plastic strain," Probl. Prochn., No. 7 (1975).
11. V. G. Vorob'ev, Heat Treatment of Steel at Temperatures below Zero [in Russian], Oborongiz, Moscow (1954).

12. A. N. Kiselev, "Magnetic measurements in shock waves," Fiz. Goreniya Vzryva, No. 6 (1975).
13. V. K. Golubev, S. A. Novikov, et al., "Mechanism of spallation of steels St. 3 and 12Kh18N10T in the temperature range 196-800°C," Probl. Prochn., No. 5 (1981).
14. V. N. German, V. I. Tsypkin, et al., "Behavior of steel Kh18N10T under the combined influence of shock loading and high-rate deformation," Probl. Prochn., No. 9 (1981).

EFFECT OF HEATING ON THE CLEAVAGE FRACTURE OF CERTAIN POLYMERIC COMPOSITES

V. K. Golubev, S. A. Novikov,
Yu. S. Sobolev, A. A. Khokhlov,
and N. A. Yukina

UDC 539.4

A successful combination of good specific mechanical properties and good thermophysical and dielectric characteristics is the reason for the broad use of polymeric composites as structural materials in high technology. However, the data available on the strength and failure of these materials under shock-wave loads is inadequate for optimizing the design of structures made of them. We can point only to the studies [1-5], which present isolated data on the conditions of cleavage failure of certain composites. There is almost no information for polymer materials on the effect of high temperature on cleavage failure, although high temperatures constitute one of the main factors affecting the service conditions of the structure. In this connection, we can cite only [6], which studied the effect of temperature on the cleavage fracture of several polymers. Here, we pose the problem of determining the conditions and character of cleavage failure of four typical polymeric composites: textolite, asbestos-textolite, glass-textolite, and glass-plastic AG-4.

The set-up of the tests was similar to [6]. The test specimens, in the form of disks 40 mm in diameter and 4 mm thick, were secured to an aluminum shield 8 mm thick. The specimens were shock-loaded by loading the shield with a 4-mm-thick aluminum plate accelerated to the required velocity by the detonation of a thin layer of explosive. The specimen was heated to 130°C through the shield by means of an electric heater. The specimen temperature was monitored with a Chromel–Alumel thermocouple. After the shock-wave tests, we visually inspected the specimens and prepared microsections of their longitudinal axial sections. The microsections were analyzed and photographed with optical equipment normally used in metallographic studies.

The methods used to obtain the materials, the conditions of their use, and their physicomechanical properties are described in [7]. Data on the density of the specimens, obtained by hydrostatic weighing, is shown in Table 1.

The test results are shown in Fig. 1 (a – textolite, b – glass-plastic, c – asbestos-plastic, d – glass-textolite). The velocity of the striker w and the temperature T correspond to the condition of the specimen after testing. The condition of the specimen was tentatively classified in accordance with three gradations: 1) absence of cleavage, correspondence of the specimen structure to the structure of the control specimen; 2) partial cleavage fracture – presence of cleavage damages visible on the microsection either unaided or at low magnification; 3) complete cleavage failure – presence of a main cleavage crack or direct separation of a cleaved layer of material. The characteristic time of mechanical loading of the specimens was 1.5 μsec, as in [6].

The estimates of the mechanical conditions of loading, characterized by the amplitude of the pressure in the compressive loading pulse, are based on the following assumptions. Table 2 gives parameters of the Hugoniot curves of certain composites in the form of linear D–u relations. The table also shows the ranges of mass velocity for which these relations were obtained. Comparison of the familiar Hugoniot curves of textolite and the binders permits us to suggest that the addition of up to 50% (by wt.) of a low-density filler such as

Moscow. Translated from Zhurnal Prikladnoi Mekhaniki i Tekhnicheskoi Fiziki, No. 6, pp. 140-145, November-December, 1987. Original article submitted September 9, 1986.

